

## Nonmagnetic Insulator State in $\text{Na}_x\text{CoO}_2$ and Phase Separation of Na Vacancies

C. de Vaulx,<sup>1</sup> M.-H. Julien,<sup>1,\*</sup> C. Berthier,<sup>1,2</sup> M. Horvatić,<sup>2</sup> P. Bordet,<sup>3</sup> V. Simonet,<sup>4</sup> D. P. Chen,<sup>5</sup> and C. T. Lin<sup>5</sup>

<sup>1</sup>Laboratoire de Spectrométrie Physique, Université J. Fourier & UMR5588 CNRS, BP 87, 38402, Saint Martin d'Hères, France

<sup>2</sup>Grenoble High Magnetic Field Laboratory, CNRS, BP 166, 38042 Grenoble Cedex 9, France

<sup>3</sup>Laboratoire de Cristallographie, CNRS, 38042 Grenoble Cedex 9, France

<sup>4</sup>Laboratoire Louis Néel, CNRS, BP 166, 38042 Grenoble Cedex 9, France

<sup>5</sup>Max-Planck-Institut for Solid State Research, Heisenbergstrasse 1, 70569 Stuttgart, Germany

(Received 17 June 2005; published 27 October 2005)

Crystallographic, magnetic, and NMR properties of a  $\text{Na}_x\text{CoO}_2$  single crystal with  $x \simeq 1$  are presented. We identify the stoichiometric  $\text{Na}_1\text{CoO}_2$  phase, which is shown to be a nonmagnetic insulator, as expected for homogeneous planes of  $\text{Co}^{3+}$  ions with  $S = 0$ . In addition, we present evidence that, because of slight average Na deficiency, chemical and electronic phase separation leads to a segregation of Na vacancies into the well-defined, magnetic,  $\text{Na}_{0.8}\text{CoO}_2$  phase. The importance of phase separation is discussed in the context of magnetic order for  $x \simeq 0.8$  and the occurrence of a metal-insulator transition for  $x \rightarrow 1$ .

DOI: 10.1103/PhysRevLett.95.186405

PACS numbers: 71.30.+h, 76.60.Cq

The discovery of superconductivity in  $\text{H}_2\text{O}$ -intercalated  $\text{Na}_{0.33}\text{Co}_2$  [1] has reopened investigations of the physical properties of  $\text{Na}_x\text{CoO}_2$  compounds, which remained largely unexplored so far. In the simplest picture, the Co planes contain  $x$  nonmagnetic ( $S = 0$ )  $\text{Co}^{3+}$  ions and  $1 - x$   $S = \frac{1}{2}$  spins ( $\text{Co}^{4+}$  low-spin state). One of the surprises in the emerging phase diagram [2] is thus the presence of magnetic order at rather low  $\text{Co}^{4+}$  concentrations  $x > 0.75$ . The origin of this order and how it evolves with  $x$  are presently unknown or controversial [3–8]. These questions are directly related to the electronic state of Co and to the microscopic organization within  $\text{CoO}_2$  layers. Their elucidation is thus necessary for understanding properties such as the remarkable thermopower of these oxides. As a matter of fact, several hypotheses have already been raised in order to rationalize magnetic order: peculiar  $\text{Co}^{3+/4+}$  charge order [6], breakdown of the  $\text{Co}^{3+/4+}$  ionic picture [7], phase separation [4,8], and/or intermediate ( $S = 1$ ) spin state for  $\text{Co}^{3+}$  [9].

In this context, a crucial question is whether the magnetic transition temperature extrapolates to zero as  $x \rightarrow 1$ , and whether this occurs in a continuous way or not. Indeed,  $\text{Na}_1\text{CoO}_2$  is usually assumed to be a nonmagnetic band insulator with fully occupied  $t_{2g}$  levels of  $\text{Co}^{3+}$  ions. This is supported by bulk susceptibility [10] and transport measurements [11]. However, chemical phase separation sometimes reported in this doping range may complicate interpretations [11,12]. Thus, investigation with a local and bulk probe, such as nuclear magnetic resonance (NMR), is clearly needed for characterizing electronic properties as  $x \rightarrow 1$ .

Here, we report NMR, x-ray, and magnetization measurements in a single crystal of  $\text{Na}_x\text{CoO}_2$  with  $x \simeq 1$ . The stoichiometric  $\text{Na}_1\text{CoO}_2$  phase is unambiguously identified and is shown to be a nonmagnetic insulator, as predicted. In addition, due to slight Na deficiency in the single crystal, we observe a distinct minority phase which has all

the crystallographic and magnetic properties of the  $x = 0.8$  phase, including a magnetic transition at low temperature ( $T$ ). We connect these results with similar observations in  $\text{Li}_x\text{CoO}_2$  [13], where phase separation might be related to the first order character of the metal-insulator transition at  $x = 0.95$  [14]. This new piece of information on electronic properties of  $\text{Na}_x\text{CoO}_2$  underlines the need for microscopic theories taking into account magnetic and metal-insulator transitions, as well as the possibility of phase separation.

We used a piece ( $3.5 \times 4.7 \times 0.45 \text{ mm}^3$ ) of a larger  $\text{NaCoO}_2$  single crystal, grown in an optical floating zone furnace [15]. NMR spectra were obtained from the sum of spin-echo Fourier transforms recorded at evenly spaced magnetic field values. Quadrupolar interaction splits each  $^{23}\text{Na}$  (resp.  $^{59}\text{Co}$ ) site into three (resp. seven) lines since the nuclear spin  $I = \frac{3}{2}$  (resp.  $\frac{7}{2}$ ). Both  $H \parallel c$ -axis and  $H \parallel ab$ -planes field orientations were investigated in order to determine quadrupolar parameters.  $^{23}\text{Na}$  shifts are given with respect to the  $^{23}\text{Na}$  resonance in  $\text{NaCl}$ . The reference for  $^{59}\text{Co}$  shift is  $10.03 \text{ MHz T}^{-1}$ . Magnetic hyperfine shift  $^{23,59}\text{K}$  data for  $H \parallel c$  were corrected from the demagnetizing field effect:  $\Delta K_c^{\text{demag}} \simeq 50 \text{ ppm}$  (resp.  $130 \text{ ppm}$ ) at  $T = 300 \text{ K}$  (resp.  $16 \text{ K}$ ).  $T_1$  values were obtained after a comb of  $\frac{\pi}{2}$  pulses.  $^{23}\text{Na}$  and  $^{59}\text{Co}$  data were fitted with appropriate formulas for magnetic relaxation and a stretched exponent  $\alpha \simeq 0.8$ – $0.9$ . For the sharp  $^{23}\text{Na}$  and  $^{59}\text{Co}$  signals,  $\alpha \neq 1$  is due to significant quadrupolar contribution to the relaxation. For the broad  $^{23}\text{Na}$  signal, the relaxation is magnetic but  $\alpha \neq 1$  because of lines with different  $^{23}T_1$  values overlap.

Figure 1(a) shows a typical  $^{23}\text{Na}$  NMR spectrum. The central line and both satellite transitions can be clearly decomposed into two contributions: (i) a sharp  $^{23}\text{Na}$  signal, with quadrupolar coupling  $\nu_Q = 1.94(1) \text{ MHz}$  and the asymmetry parameter of the electric field gradient tensor  $\eta = |V_{xx} - V_{yy}|/V_{zz} = 0$ , in reasonable agreement with room  $T$  data [16]. The full width at half maximum

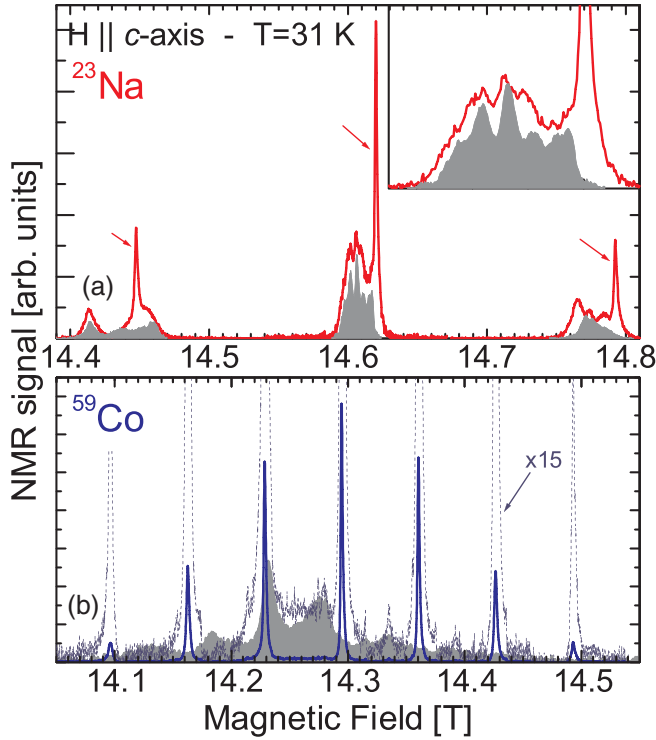


FIG. 1 (color online). (a)  $^{23}\text{Na}$  NMR spectrum, showing the sharp (arrows) and broad signals. Experimental conditions were chosen in order to favor the broad signal. The sharp lines are thus comparatively much more intense than shown here. The gray area is the  $^{23}\text{Na}$  NMR spectrum in a  $\text{Na}_{0.8}\text{CoO}_2$  single crystal [18]. Inset: detail of the  $^{23}\text{Na}$  central lines for  $x = 1$  and  $x = 0.8$  crystals. Note that the number of  $^{23}\text{Na}$  NMR lines and their shifts may somewhat vary from sample to sample with  $x \approx 0.8$  [18], so that strict one-to-one correspondence of  $^{23}\text{Na}$  NMR lines is not required to identify the  $x \approx 0.8$  phase here. (b)  $^{59}\text{Co}$  NMR spectrum in full scale (line) and in enlarged scale (dashed line) in order to evidence the broad  $^{59}\text{Co}$  signal. Grey area:  $^{59}\text{Co}$  NMR spectrum for  $x = 0.8$  [18].

(FWHM) at  $T = 50$  K is 17 kHz at 14.6 T and 13.4 kHz at 8.5 T, mostly due to nuclear dipolar broadening. Such a very small magnetic and quadrupolar broadening indicates that this single Na site must be in a very well-ordered structure. The magnetic hyperfine shift of this line is negligibly small:  $^{23}K_c^{\text{sharp}} < 35$  ppm over the whole temperature ( $T$ ) range (Fig. 2). This sharp  $^{23}\text{Na}$  signal exactly corresponds to what is expected for  $\text{Na}_1\text{CoO}_2$ : at variance with other concentrations, this stoichiometric phase is characterized by a single Na crystallographic site [17], with axial symmetry (thus  $\eta = 0$ ), and supposedly 100%  $\text{Co}^{3+}$  occupation (thus a vanishing hyperfine field on  $^{23}\text{Na}$ ). (ii) A broader signal, corresponding to a more disordered structure, consists of at least three contributions. Quadrupolar parameters [ $\nu_Q = 1.78(5)$ ,  $1.85(5)$ , and  $2.08(5)$  MHz and  $\eta \approx 0$ ] are similar to the sharp signal. Since the relative positions of the central lines scale with the magnetic field, the second-order quadrupolar shift is negligible and the shift differences between these lines are

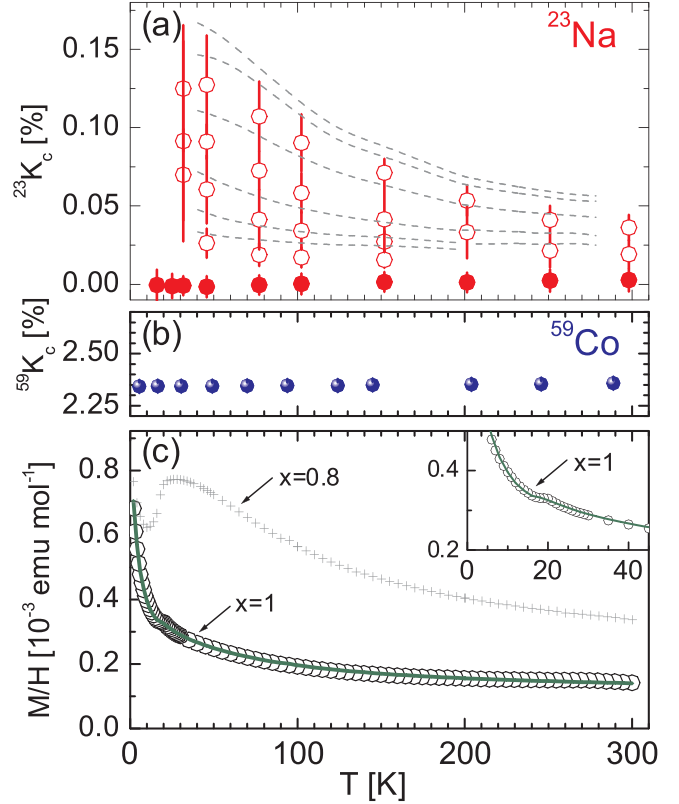


FIG. 2 (color online). (a)  $^{23}\text{Na}$  magnetic hyperfine shift for  $H \parallel c$  ( $^{23}K_c$ ) for the sharp (filled symbols) and broad (open symbols) signals. Vertical bars are not error bars but the FWHM. Dashed lines:  $^{23}K_c$  in  $\text{Na}_{0.8}\text{CoO}_2$  [18]. (b)  $^{59}K_c$  for the sharp  $^{59}\text{Co}$  signal. FWHM is close to the symbol size. (c) Symbols: magnetization data ( $H = 1$  T,  $\parallel c$ ). Line: fit explained in the text. Inset: same data in enlarged scale showing a hump at  $T_M = 20$  K.

only due to the number of different magnetic environments for  $^{23}\text{Na}$  nuclei. All shift values  $^{23}K_c^{\text{broad}}$  at any  $T$  are remarkably close to those in a  $\text{Na}_{0.8}\text{CoO}_2$  single crystal [18] (Fig. 1), with the Curie-Weiss  $T$  dependence typical of the spin susceptibility for  $x > 0.6$  samples (Fig. 2).

Information on the magnetic fluctuations for the two sets of signals can be obtained through site-selective measurements of nuclear spin-lattice and spin-spin relaxation rates,  $T_1^{-1}$  and  $T_2^{-1}$ , respectively. The two  $^{23}\text{Na}$  signals clearly display very different behaviors:

$^{23}T_1$  for the sharp line is extremely long, more than 20 s at any  $T$  (Fig. 3). Such long  $^{23}T_1$  values indicate that the spectral weight of magnetic fluctuations almost vanishes at the nuclear Larmor frequency. This result is again very consistent with a nonmagnetic insulator, as expected for low-spin  $\text{Co}^{3+}$  forming the  $\text{Na}_1\text{CoO}_2$  phase. Indeed, the presence of magnetic moments within  $\text{CoO}_2$  layers would speed up relaxation noticeably. Since delocalized electronic wave functions would significantly overlap with Na orbitals, a nonmagnetic metallic phase would also cause much faster relaxation with typically  $^{23}T_1^{-1} \propto T$ , in contrast with our findings. The very slow spin-lattice

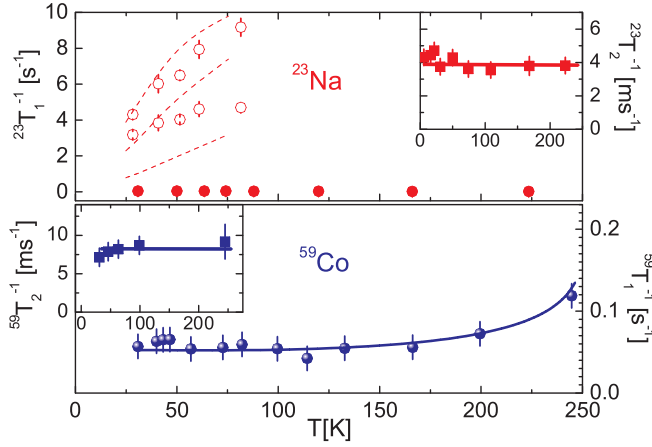


FIG. 3 (color online). Top:  $T_1^{-1}$  data for the broad (open symbols) and sharp (filled symbols)  $^{23}\text{Na}$  signals. For the latter,  $T_1$  could be reliably extracted at two different positions only on the broad spectrum, while  $^{23}T_1$  in  $\text{Na}_{0.8}\text{CoO}_2$  (dashed lines) could be measured for three resolved groups of lines [18]. Inset:  $T_2^{-1}$  for the sharp  $^{23}\text{Na}$  signal. Bottom:  $T_1^{-1}$  and  $T_2^{-1}$  (inset) for the sharp  $^{59}\text{Co}$  signal. Continuous lines are guides to the eye.

relaxation observed here is thus phase specific. As a matter of fact, such large  $^{23}T_1$  values are not observed on any  $^{23}\text{Na}$  line in  $\text{Na}_{0.8}\text{CoO}_2$  [18], which also contains a large number of  $\text{Co}^{3+}$  ions.

For the broad signal, on the other hand, both the magnitude and the  $T$  dependence of  $^{23}T_1^{-1}$  are very close to those measured on  $^{23}\text{Na}$  lines in a  $\text{Na}_{0.8}\text{CoO}_2$  single crystal [18] (Fig. 3). This result nicely fits with shift data attributing this signal to a Na-deficient phase.

The characteristic time  $^{23}T_2$  of the spin-echo decay for the sharp signal is roughly constant in the whole  $T$  range (Fig. 3). For the broad signal, however, the spin-echo decay shows a complex behavior (to be analyzed in a forthcoming publication) below  $\sim 20$  K, which is the hallmark of the magnetic ordered state in  $\text{Na}_{0.8}\text{CoO}_2$  [18]. The occurrence of magnetic order at  $T_M = 20$  K definitely ensures that we are dealing with the  $x \approx 0.8$  phase.

The  $^{23}\text{Na}$  signal intensity, integrated over magnetic field values and corrected for  $T_1$  and  $T_2$  effects, is proportional to the number of nuclei in each phase. Here, we measure a ratio of the broad to sharp  $^{23}\text{Na}$  signals of 1:6 for both the central transition and the satellites. This is thus considered as the volume ratio of the two phases. Remarkably, this ratio is confirmed by measurements of the bulk magnetization using a superconducting quantum interferometer device (SQUID):  $M/H$  data for  $H \parallel c$  can be fitted with a constant term of  $7.6 \times 10^{-5} \text{ emu} \cdot \text{mol}^{-1}$ , a Curie-Weiss term  $\frac{0.0031}{T+4}$  due to 0.8% impurities in the crystal, plus  $\frac{1}{7}$  of the magnetization measured in a  $\text{Na}_{0.8}\text{CoO}_2$  single crystal [Fig. 2(c)]. This last contribution accounts for the small hump at  $T_M \approx 20$  K discernible in the raw data.

Since  $T_M$  is known to be zero for  $x < 0.75$ , 20–22 K for  $x = 0.75\text{--}0.82$  [3,18], and 27 K for  $x = 0.85$  [5], we

assume the Na concentration of the Na-poor phase:  $x_2 \approx 0.8\text{--}0.9$ . With  $x_2 = 0.8$  (resp. 0.9) and the 1:6 intensity ratio, we estimate the average Na concentration  $x_{\text{av}} = 0.97$  (resp. 0.98) in this single crystal.

The  $^{23}\text{Na}$  NMR results are also corroborated by  $^{59}\text{Co}$  NMR: a typical  $^{59}\text{Co}$  NMR spectrum [Fig. 1(b)] is composed of the expected seven lines, each of them being extremely sharp (FWHM of 15 kHz at 14.3 Tesla for the central line) and split by  $\nu_Q = 0.68(2)$  MHz. This indicates a single Co site, again in a very well-ordered crystallographic and electronic structure, with axial symmetry derived from the asymmetry parameter  $\eta = 0$ . The shift  $^{59}K^{\text{sharp}}$  for this site is entirely attributed to the  $T$  independent orbital term  $^{59}K_c^{\text{orb}} = 2.35\%$  and  $^{59}K_{ab}^{\text{orb}} = 2.11\%$  (similar values are found for  $\text{Co}^{3+}$  sites in  $\text{Na}_{0.7}\text{CoO}_2$ , after correcting for the reference choice) [19]; i.e., the spin contribution is negligible (Fig. 2).  $^{59}T_1^{\text{sharp}}$  is again extremely long over the whole  $T$  range [much longer than in  $\text{Na}_{0.3}\text{CoO}_2$  [20]] and  $^{59}T_2^{\text{sharp}}$  is almost  $T$  independent (Fig. 3). This sharp  $^{59}\text{Co}$  signal, whose properties are identical to those of the sharp  $^{23}\text{Na}$  signal, is undoubtedly attributed to the  $x = 1$  phase. The absence of magnetism in  $\text{CoO}_2$  layers is thus confirmed:  $\text{Na}_1\text{CoO}_2$  is the predicted band insulator. Note also that the long  $^{23}T_1$  and  $^{59}T_1$  values are indicative of the high purity of the  $\text{Na}_1\text{CoO}_2$  phase in our sample.

In addition to the sharp signal, the  $^{59}\text{Co}$  NMR spectrum also features a broad contribution (Fig. 1) with larger shift, which is very reminiscent of the  $^{59}\text{Co}$  signal in  $\text{Na}_{0.8}\text{CoO}_2$  [18]. However, the weak integrated intensity of this signal (consistent with the intensity ratio for  $^{23}\text{Na}$  signals) and its large broadening prevented us from accurate relaxation measurements.

The sample was also characterized by x-ray diffraction using a Seifert texture goniometer with  $\text{Cu } \lambda K\alpha$  radiation. The crystal was mounted in symmetric reflection geometry with the scattering vector perpendicular to the crystal plate surface and therefore expected to be parallel to the  $c^*$  axis. A  $\theta$ - $2\theta$  scan showed markedly split  $(00\ell)$  reflections around  $2\theta = 17^\circ$  and  $34^\circ$ , indicating the existence of two phases in the crystal. Measurements of the  $(003)_R$  and  $(006)_R$  reflections [rhombohedral unit cell, or  $(002)_H$  and  $(004)_H$  for the corresponding hexagonal cell] allowed us to determine  $c$ -axis parameters. For rhombohedral (resp. hexagonal) cells:  $c_1 = 16.044(5)$  Å (resp. 10.696) for phase 1 is identical to the  $c$  value in  $\text{Na}_{0.8}\text{CoO}_2$  [12], and  $c_2 = 15.594(5)$  Å (resp. 10.395) for the majority phase 2 is the value found in  $\text{Na}_1\text{CoO}_2$  [17]. Thus, our single crystal shows chemical phase separation between  $x = 0.8$  and  $x = 1$  phases, in agreement with the results of Huang *et al.* in  $\text{Na}_{0.89}\text{CoO}_2$  [12].

It must be stressed that the observation of two phases is different from trivial inhomogeneity, such as variation of the Na content along the growth direction or gradual Na loss from the crystal's surface. This would result in NMR line broadening, at variance with the two distinct phases

identified here. Our observation of well-defined phases, together with the absence of time evolution of NMR (and SQUID) results, demonstrates that NMR probes the bulk of the single crystal and is therefore not sensitive to possible surface degradation [21]. This does not exclude that the Na deficiency may partially result from losses at the surface after the crystal synthesis, but our results reveal that Na vacancies must segregate at some point.

Actually, several works suggest that  $\text{Na}_x\text{CoO}_2$  compounds tend to phase separate between stable, well-defined, Na concentrations [11,12,22]. In particular, a miscibility gap between  $x = 0.8$  and  $x = 1$  phases is suggested by the results of Huang *et al.* [12]. Such a chemical phase separation would straightforwardly explain the electronic phase separation evidenced here.

On the other hand, an important point to be considered is that similar phase separation is clearly established in  $\text{Li}_x\text{CoO}_2$ , which has the same  $\text{CoO}_2$  layers as  $\text{Na}_x\text{CoO}_2$  but different Li stacking sequence. Experiments have demonstrated that  $\text{Li}_x\text{CoO}_2$  separates into Li-rich and Li-poor phases, over a large concentration range  $0.75 \leq x \leq 0.94$  [13]. Furthermore, theoretical calculations and the fact that the two phases have identical crystallographic structure (unlike Na compounds) have led to the suggestion that phase separation is not driven by Li vacancy ordering [13,23]. Because of the concomitance of a metal-insulator transition at  $x = 0.95$ , electronic delocalization is proposed as the driving force for phase separation [13]. According to Marianetti *et al.*, this transition is actually a Mott transition within the impurity band of Li vacancies and its first order nature would explain electronic phase separation [14]. The high  $\text{Li}^+$  mobility in this system would then allow global, chemical, phase separation to proceed. Since there must be a metal-insulator transition between  $x = 0.9$  and  $x = 1$  in  $\text{Na}_x\text{CoO}_2$  as well, similar physics is expected to be at work in this system. Another remarkable fact is that phase separation is clearer in clean  $\text{Li}_x\text{CoO}_2$  samples than in impurity-doped ones [24]. This tends to reinforce the conclusion that phase separation is an intrinsic phenomenon in these oxides.

Deciding whether the origin of phase separation is electronic or chemical is beyond the scope of our work, which shows that both occur. Identification of the sequence of stable phases is now clearly needed and a possible dependence on the synthesis conditions/methods should be clarified as well. Spatially inhomogeneous electronic states and anomalous magnetism might be the two key features to be considered for explaining thermopower, which is actually strongest in this doping range. These progresses should thus stimulate theoretical activity towards microscopic models, specifically for the high doping region from  $x = 0.75$  up to the metal-insulator transition.

Returning back to the magnetic properties of  $\text{Na}_x\text{CoO}_2$ , the fact that the Na-poor phase has a concentration  $x \approx 0.8$  does not support the hypothesis [4,8] that this phase is itself phase separated. As to the proposal that a certain amount of

$\text{Co}^{3+}$  sites are in an intermediate spin state ( $S = 1$ ) [9], no definitive conclusion can be drawn from the present NMR results. Although our data rule out the presence of  $S = 1$  spins in the  $x = 1$  phase, *local* changes of the  $\text{Co}^{3+}$  spin state close to local lattice deformations (induced by a putative  $\text{Co}^{3+}/\text{Co}^{4+}$  pattern) cannot be excluded in  $x \approx 0.8$  phases. However, it remains to be seen whether magnetization data, which have been explained by a concentration  $x$  of  $S = \frac{1}{2}$  spins [3], could support  $S = 1$  moments as well.

We wish to thank H. Mayaffre for his constant support and fruitful discussions.

*Note added.*—Recently reported NMR spectra for the  $\text{Na}_1\text{CoO}_2$  phase [G. Lang *et al.*, Phys. Rev. B **72**, 094404 (2005)] quantitatively agree with ours.

---

\*Email address: Marc-Henri.Julien@ujf-grenoble.fr

- [1] K. Takada *et al.*, Nature (London) **422**, 53 (2003).
- [2] M. L. Foo *et al.*, Phys. Rev. Lett. **92**, 247001 (2004).
- [3] T. Motohashi *et al.*, Phys. Rev. B **67**, 064406 (2003); J. Sugiyama *et al.*, Phys. Rev. B **67**, 214420 (2003); S. Bayrakci *et al.*, Phys. Rev. B **69**, 100410 (2004); J. Sugiyama *et al.*, Phys. Rev. B **69**, 214423 (2004); B. C. Sales *et al.*, Phys. Rev. B **70**, 174419 (2004); J. L. Luo *et al.*, Phys. Rev. Lett. **93**, 187203 (2004); J. Wooldridge *et al.*, J. Phys. Condens. Matter **17**, 707 (2005); D. Prabhakaran *et al.*, cond-mat/0312493.
- [4] H. Sakurai *et al.*, J. Phys. Soc. Jpn. **73**, 2081 (2004).
- [5] P. Mendels *et al.*, Phys. Rev. Lett. **94**, 136403 (2005).
- [6] S. P. Bayrakci *et al.*, Phys. Rev. Lett. **94**, 157205 (2005).
- [7] L. H. Helme *et al.*, Phys. Rev. Lett. **94**, 157206 (2005).
- [8] P. Carretta *et al.*, Phys. Rev. B **70**, 024409 (2004).
- [9] C. Bernhard *et al.*, Phys. Rev. Lett. **93**, 167003 (2004).
- [10] S. Kikkawa, S. Miyazaki, and M. Koizumi, J. Solid State Chem. **62**, 35 (1986).
- [11] C. Delmas *et al.*, Solid State Ionics **3–4**, 165 (1981).
- [12] Q. Huang *et al.*, Phys. Rev. B **70**, 184110 (2004).
- [13] M. Ménétrier *et al.*, J. Mater. Chem. **9**, 1135 (1999), and references therein.
- [14] C. A. Marianetti, G. Kotliar, and G. Ceder, Nat. Mater. **3**, 627 (2004).
- [15] D. P. Chen *et al.*, Phys. Rev. B **70**, 024506 (2004).
- [16] R. Siegel *et al.*, Solid State Nucl. Magn. Reson. **23**, 243 (2003).
- [17] Y. Takahashi, Y. Gotoh, and J. Akimoto, J. Solid State Chem. **172**, 22 (2003).
- [18] C. de Vaulx *et al.* (unpublished).
- [19] I. R. Mukhamedshin *et al.*, Phys. Rev. Lett. **94**, 247602 (2005).
- [20] F. L. Ning *et al.*, Phys. Rev. Lett. **93**, 237201 (2004).
- [21] When not in the cryostat, the sample was stored in liquid  $\text{N}_2$  in order to prevent surface degradation in air.
- [22] Q. Huang *et al.*, J. Phys. Condens. Matter **17**, 1831 (2005).
- [23] A. van der Ven *et al.*, Phys. Rev. B **58**, 2975 (1998).
- [24] H. Tukamoto and A. R. West, J. Electrochem. Soc. **144**, 3164 (1997).